Inorganic Chemistry

Article

pubs.acs.org/IC

Synthesis, Structure, and Paramagnetism of Manganese(II) Iminophosphate Complexes

Daniel N. Woodruff,[†] Eric J. L. McInnes,[†,‡] Daniel O. Sells,[†,‡] Richard E. P. Winpenny,[†,‡] and Richard A. Layfield*,[†]

[†]School of Chemistry, The University of Manchester, Oxford Road, Manchester, M13 9PL, United Kingdom

[‡]EPSRC U.K. National EPR Facility, Photon Science Institute, The University of Manchester, Oxford Road, Manchester, M13 9PL, United Kingdom

S Supporting Information

ABSTRACT: The coordination chemistry of the bidentate bis(imino)bis(amino)phosphate ligands $[\mathrm{Me_3SiN{=}P\{NR\}\{N(H)R\}_2}]^-$, where R = *n*-propyl is $[\mathrm{L^1H_2}]^-$, R = cyclohexyl is $[\mathrm{L^2H_2}]^-$, and R = *tert*-butyl is $[\mathrm{L^3H_2}]^-$, with manganese(II), is described. The bis(imino)bis(amino)phosphate-manganese(II) complexes $[(\eta^5\text{-Cp})\mathrm{Mn}(\mu\text{-L^1H_2})]_2$ (**1**), $[\mathrm{Mn(L^2H_2)_2}]\cdot\mathrm{THF}$ (**2**·THF), and $[(\eta^5\text{-Cp})\mathrm{Mn(L^3H_2)}]$ (**3**) were synthesized by monodeprotonation of the respective pro-ligands by manganocene, $\mathrm{Cp_2Mn}$. The molecular structures of **1**−**3** reveal that the steric demands of the ligand N-substituents play a dominant role in determining the aggregation state and overall composition of the manganese(II) complexes. The coordination geometries of the Mn(II) centers are six-coordinate pseudotetrahedral in **1**, four-coordinate distorted tetrahedral in **2**, and five-coordinate in **3**, resulting in formal valence electron counts of 17, 13, and 15, respectively. EPR studies of **1**−**3** at Q-band reveal high-spin manganese(II) ($S = {}^5/_2$) in each case. In the EPR spectrum of **1**, no evidence of intramolecular magnetic exchange was found. The relative magnitudes of the axial zero-field splitting parameter, D, in **2** and **3** are consistent with the symmetry of the manganese environment, which are D_{2d} in **2** and C_{2v} in **3**.

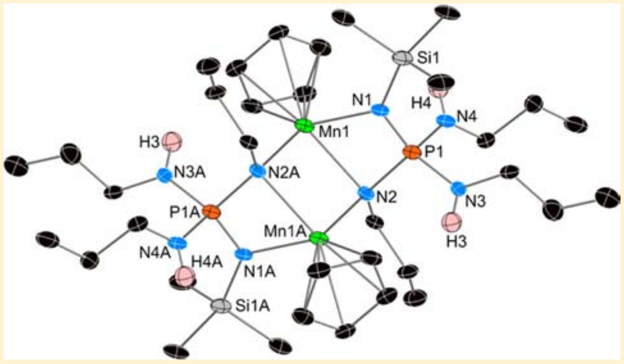

Oxygen-donor ligands centered on phosphorus(V), such as phosphate and phosphonates, display extremely rich coordination chemistry.[1,2] Organophosphonate ligands of the type $[\mathrm{RPO_3}]^{2-}$ have been widely applied in transition metal and main group metal chemistry to develop, for example, porous metal−organic frameworks (MOFs).[3] The diverse range of phosphonate coordination modes has also enabled the synthesis of an array of polymetallic phosphonate-bridged cage compounds of 3d transition metals, some of which possess interesting magnetic properties, such as the ability to act as magnetic coolants.[4] Imino analogues of phosphate and phosphonate ligands, in which up to four oxygen atoms are notionally replaced by isoelectronic imino (NR) groups, have also attracted considerable interest owing to the potential changes in chemical and physical properties that these ligands can introduce relative to related compounds with simple phosphonate ligands.[5] The family of phosphorus(V)-imino ligands include tris(imino)phosphates, and their thio and seleno versions, and the tetrakis(imino)phosphates,[6,7] all of which are known in mono-, di-, and trianionic forms represented by $[\mathrm{E{=}P\{N(H)R\}_{3-\mathit{n}}\{NR\}_\mathit{n}}]^{n-}$ (n = 1−3; E = $\mathrm{NSiMe_3}$, O, S, Se; R = alkyl or aryl).

The development of phosphorus(V)-imino ligands was pioneered by Chivers and co-workers.[5,6] Detailed studies of phosphorus(V)-imino complexes of s-block metals, zinc, and aluminum have established the fundamental properties of these ligands, and revealed that the structures and reactivity of their complexes depend on a range of factors. Notably, the imino N-substituents strongly influence the extent to which the ligand precursor can be deprotonated, and it was also found that the spatial demands of the N-substituents play an important role in determining cage nuclearity in the solid state.[5−7] In contrast to their coordination chemistry with main group metals, transition metal complexes of phosphorus(V)-imino ligands are very rare. Indeed, only one phosphorus(V)-imino ligand has been used in transition metal chemistry, namely, the monoanionic (imino)-thiophosphate $[\mathrm{S{=}P\{N(H)R\}_2\{NR\}}]^-$ (**L**), for which complexes of molybdenum(VI), rhodium(I), and nickel(II) are known, although no studies on the paramagnetism of the distorted tetrahedral nickel(II) complex $[\mathrm{Ni(\mathbf{L})_2}]$ were reported.[8]

The paucity of transition metal complexes of phosphorus(V)-imino ligands, particularly of paramagnetic ions, has prompted us to develop the coordination chemistry of ligands derived from the tris(amino)phosphoranes $[\mathrm{Me_3SiN{=}P\{N(H)R\}_3}]$, where R = *n*-propyl ($\mathrm{L^1H_3}$), cyclohexyl ($\mathrm{L^2H_3}$), or *tert*-butyl ($\mathrm{L^3H_3}$). Our choice of transition metal ion was

Received: June 29, 2012
Published: August 9, 2012

dx.doi.org/10.1021/ic3014046 | *Inorg. Chem.* 2012, 51, 9104−9109

determined by our previous studies on manganese(II) amido/imido cage compounds, which can be synthesized conveniently by direct deprotonation (manganation) of simple aromatic amines by bis(cyclopentadienyl)manganese(II) (manganocene, Cp_2Mn).[9,10] The primary, secondary, and tertiary alkyl substituents on the amino nitrogens in L^nH_3 were chosen to allow the effects of increasing steric bulk to be investigated. Thus, we now report the synthesis, structures, and EPR spectroscopic properties of the manganese(II) complexes $[(\eta^5\text{-Cp})Mn(\mu\text{-}L^1H_2)]_2$ (**1**), $[Mn(L^2H_2)_2]\cdot THF$ (**2**·THF), and $[(\eta^5\text{-Cp})Mn(L^3H_2)]$ (**3**).

RESULTS AND DISCUSSION

Synthetic and Structural Studies. The syntheses of ligands L^2H_3 and L^3H_3 have been reported previously,[6b] whereas we have developed L^1H_3 for our current study. Complexes **1**–**3** were synthesized by direct manganation of the corresponding pro-ligand L^nH_3 in toluene or THF solvent, according to Scheme 1. Single crystals of **1**–**3** were obtained by slow cooling of saturated solutions of each compound in its reaction solvent, and their structures were determined by X-ray diffraction. Solutions of **1**–**3** in their respective reaction solvents are stable for the duration of the synthesis, although heating the solutions to reflux even for brief periods results in decomposition to insoluble brown material. Crystalline samples of **1**–**3** are stable at room temperature in a glovebox for two weeks, before gradual decomposition becomes apparent.

Scheme 1. Synthesis of 1–3

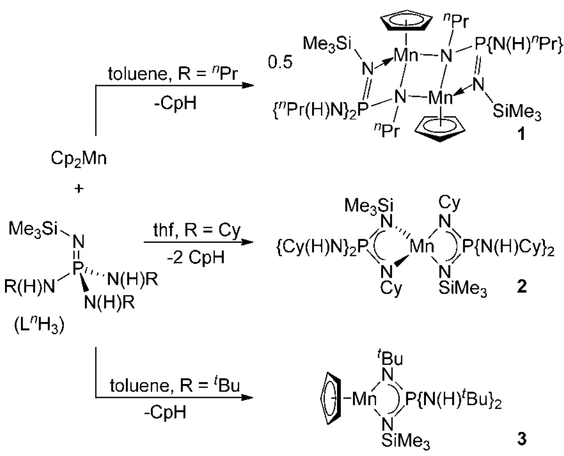

The dimer $[(\eta^5\text{-Cp})Mn(\mu\text{-}L^1H_2)]_2$ (**1**) crystallized as extremely air-sensitive green blocks, in an isolated yield of 60%. Molecules of **1** are located about a crystallographic inversion center, which coincides with the midpoint of the Mn(1)···Mn(1A) axis (Figure 1). The molecular structure of the dimer consists of two manganese centers μ-bridged by the amido nitrogen atoms formally deprotonated in the synthesis of **1**, resulting in Mn(1)–N(2) and Mn(1)–N(2A) bond lengths of 2.316(4) and 2.167(4) Å, respectively. The resulting N(2)–Mn(1)–N(2A) and Mn(1)–N(2)–Mn(1A) angles are 94.85(14)° and 85.14(14)°, respectively. The trimethylsilylimino nitrogen N(1) bonds in a terminal manner to Mn(1), giving an Mn(1)–N(1) bond length of 2.183(4) Å and N(1)–Mn(1)–N(2) and N(1)–Mn(1)–N(2A) angles of 63.38(14)° and 104.69(15)°, respectively. The P(1)–N(1) distance in **1** is 1.588(4) Å whereas the P(1)–N(2) distance is 1.637(4) Å, indicating that the formal negative charge in the $[L^1H_2]^-$ ligand is localized on N(2) in order to allow more effective μ-bridging between the manganese centers. The coordination environment of each manganese in **1** is completed by an η^5-cyclopentadienyl ligand, with the Mn–C bond lengths of 2.469(5)–2.600(5) Å implying a high-spin $S = {}^5/_2$ configuration at Mn(II) (see EPR Spectroscopy section, below). The manganese centers in **1** occupy a pseudotetrahedral or "piano-stool" coordination geometry, and they have a formal valence electron count of 17.

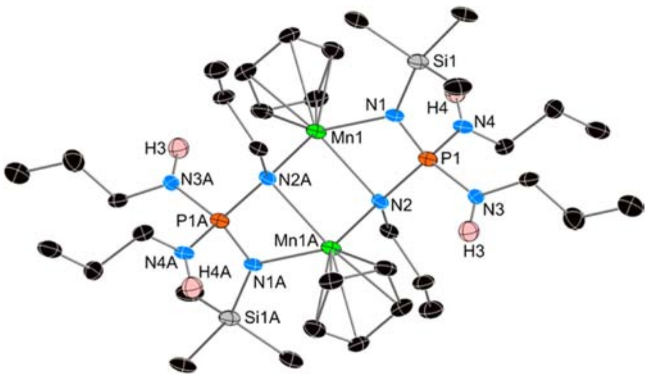

Figure 1. Thermal ellipsoid representation (50% probability) of the molecular structure of $[(\eta^5\text{-Cp})Mn(\mu\text{-}L^1H_2)]_2$ (**1**). Unlabeled atoms are carbon (black). For clarity, hydrogen atoms, except those bonded to nitrogen, are omitted.

The reaction of manganocene and L^2H_3 produced the same outcome irrespective of the relative amounts of Cp_2Mn and pro-ligand in the reaction mixture, producing $[Mn(L^2H_2)_2]\cdot THF$ (**2**·THF) as pale-brown needles. Placing samples of **2**·THF under vacuum for about 30 min removed the THF of crystallization, allowing **2** to be isolated in a yield of 56%. In the crystal structure of **2**·THF, equivalent atoms are related by a crystallographic 2-fold rotation axis that passes through Mn(1) and runs parallel to the *b*-axis. The molecular structure of **2** reveals that the manganese center resides in a very distorted tetrahedral environment, formed by four nitrogen donors from two $[L^2H_2]^-$ ligands (Figure 2), which produces a valence electron count of 13. The $[L^2H_2]^-$ ligands in **2** are κ^2-coordinated to Mn(1) through one nitrogen bearing a cyclohexyl substituent and another bearing a trimethylsilyl

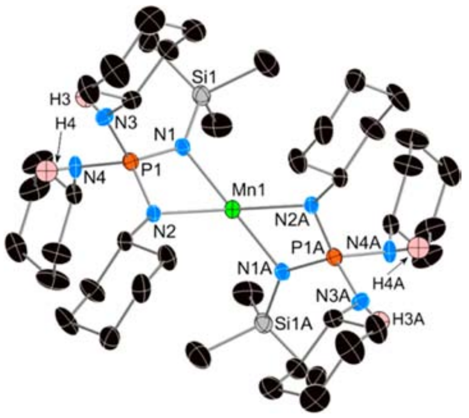

Figure 2. Thermal ellipsoid representation (50% probability) of the molecular structure of $[Mn(L^2H_2)_2]\cdot THF$ (**2**·THF), viewed along the crystallographic *b*-axis. Unlabeled atoms are carbon (black). For clarity, hydrogen atoms, except those bonded to nitrogen, are omitted.

substituent, which produces Mn(1)−N(1) and Mn(1)−N(2) bond distances of 2.085(3) and 2.149(3) Å, respectively. The distorted nature of the tetrahedral Mn(1) environment is clearly revealed by the N−Mn(1)−N angles, which are in the range 71.2(1)−135.0(2)° (average 116.6°). The dihedral angle between the N(1)−Mn(1)−N(2) and N(1A)−Mn(1)−N(2A) planes in **2** is 87.9(2)°. The P(1)−N(1) and P(1)−N(2) distances of 1.596(8) and 1.601(6) Å are essentially the same (within crystallographic uncertainty), suggesting that the formal negative charge of the ligand is delocalized equally onto both nitrogen donor atoms, and that the different lengths of the Mn−N bonds in **2** are probably due to steric interactions between the substituents.

The 1:1 stoichiometric reaction of Cp_2Mn and L^3H_3 produced $[(\eta^5\text{-}Cp)Mn(L^3H_2)]$ (**3**) as amber crystals, in a yield of 35%. In the half-sandwich complex **3** (Figure 3), a pseudo-three-coordinate manganese(II) center is complexed by a κ^2-$[L^3H_2]^-$ ligand and an η^5-Cp ligand, which produces a valence electron count of 15.

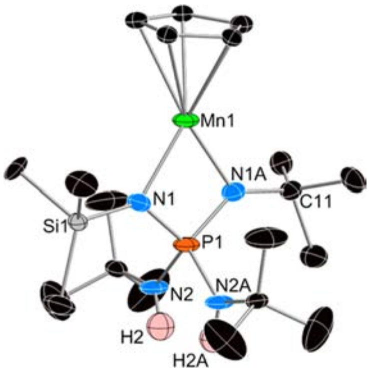

Figure 3. Thermal ellipsoid representation (30% probability) of the molecular structure of $[(\eta^5\text{-}Cp)Mn(L^3H_2)]$ (**3**). Unlabeled atoms are carbon (black). For clarity, hydrogen atoms, except those bonded to nitrogen, are omitted.

Compound **3** crystallizes in the space group *Pmmn*. The crystallographic mirror plane running parallel to the *c*-axis, in which Mn(1), N(2), and N(2A) lie, results in the $NSiMe_3$ group and the N^tBu group containing N(1) being disordered over equivalent sites, with equal occupancies, meaning that they cannot be distinguished from each other in the crystal structure. The second mirror plane, parallel to the crystallographic *a*-axis, passes through Mn(1), Si(1), and C(11): the two mirror planes also coincide at the center of the η^5-Cp ligand; hence, each of these carbon atoms is disordered over four sites. The Mn−N(1) distance in **3** is 2.073(5) Å, which as expected is similar to the analogous distances in **2**, but is considerably shorter than the Mn−N distances in **1**. The P(1)−N(2) distance of 1.669(5) Å in **3** is approximately 0.07 Å longer than the P(1)−N(1) distance of 1.601(5) Å, and indicates that the formal negative charge on the $[(L^3H_2)]^-$ ligand is delocalized across an N(1)−P(1)−N(1A) π-system, as observed in **2**. The range of Mn−C distances in **3** is 2.393(17)−2.415(17) Å, suggesting high-spin manganese(II).

Compounds **1**−**3** are the first transition metal complexes of an imino-phosphorane ligand, and they are very rare examples of d-block complexes of imino-analogues of phosphate and organophosphonate ligands. The synthesis of **1**−**3** highlights that manganocene is indeed capable of singly deprotonating the L^nH_3 pro-ligands; however, multiple deprotonations of one pro-ligand by manganocene are apparently not possible under the conditions used. The reasons for the selective monodeprotonations may be due in part to the fact that we have employed aliphatic N-substituents, which would result in the N−H bonds in L^nH_3 having lower thermodynamic acidity relative to analogues of these ligands with aryl substituents. This idea is broadly consistent with a study of the reactions of Cp_2Mn with N-aryl primary amines and with *N,N′*-dibenzylethylenediamine, which resulted in deprotonation in the former instance and simple complexation by the diamine in the second instance.[10b]

The most notable contrast in the synthesis and structures of **1**−**3** is that the outcome seemingly depends on the steric demands of the N-alkyl substituent: as the alkyl substituent changes from primary to secondary and then to tertiary in **1**, **2**, and **3**, respectively, the coordination number of manganese changes from six to four to five. In the absence of sterically demanding substituents, mono(cyclopentadienyl)manganese(II) complexes typically adopt pseudotetrahedral, piano-stool geometries, resulting in 17-electron complexes of the type $[(\eta^5\text{-}Cp)MnX(L)_2]$ (X = anionic ligand, L = neutral two-electron donor).[9−12] The typical piano-stool geometry is achieved in the dimer **1** via the μ-bridging amido group within the $[L^1H_2]^-$ ligand, which carries sterically nondemanding *n*-propyl substituents. In contrast, the *t*-butyl group in **3** precludes dimerization on steric grounds. Comparing the structures of **1** and **3** with that of **2** must be done cautiously because **2** was synthesized in THF solvent, as opposed to toluene for **1** and **3**. Indeed, the effects of using THF are potentially significant because polar aprotic solvents coordinate to the manganese(II) center in Cp_2Mn and lengthen the Mn−C bonds,[13] which conceivably labilize the Cp ligands toward metalation of N−H acidic substrates. This analysis can explain why both Cp ligands were cleaved in the reaction of Cp_2Mn with L^2H_3, whereas in toluene only one Cp ligand was cleaved in the reactions of Cp_2Mn with L^1H_3 and with L^2H_3.

EPR Spectroscopy. Q-band EPR spectra of polycrystalline samples of **1**−**3** were recorded in order to investigate the electronic structure of the manganese(II) centers. In each case, the spectra at low temperature are rich, and they exhibit extensive fine structure (Figure 4), which can be modeled accurately on the basis of isolated $S = {}^5/_2$ centers, hence confirming the high-spin nature of the Mn(II) ions. This gave the following axial (*D*) and rhombic (*E*) zero-field splitting (ZFS) parameters: $D = +0.11$ and $E = 0.005\ cm^{-1}$ for **1**; $D = -0.12$ and $E = 0.005\ cm^{-1}$ for **2**; $D = +0.49$ and $E = 0.078\ cm^{-1}$ for **3**. In each case an isotropic *g*-value of 2.00 was used, and because the relative intensities of the features in EPR spectra are sensitive to the sign of *D*, the values were determined by comparing simulations with negative and positive *D*.

Compared to **1** and **2**, there are two notable features in the EPR data for complex **3**: the ZFS (*D*) of the $S = {}^5/_2$ ion in **3** is much greater, as is the rhombicity parameter $|E/D|$ [which can take values between 0 (axial) and ${}^1/_3$ (the rhombic limit) in the usual definition]. The relative magnitudes of $|D|$ in the monometallic complexes **3** and **2** are consistent with the local coordination geometries, which is distorted tetrahedral (D_{2d}) $\{MnN_4\}$ in **2**, and formally five-coordinate, pseudo-three-coordinate (C_{2v}) $\{CpMnN_2\}$ in **3**. Furthermore, if, as expected, the local ligand field in **3** is dominated by the Mn−Cp(centroid) axis (defining a local *z*-direction), then the two in-plane (*x*, *y*) directions (in and perpendicular to the $\{MnN_2\}$ plane) are very different, hence giving a large $|E/D|$. The EPR spectra for dimer **1** are very similar to those of monometallic **2**.

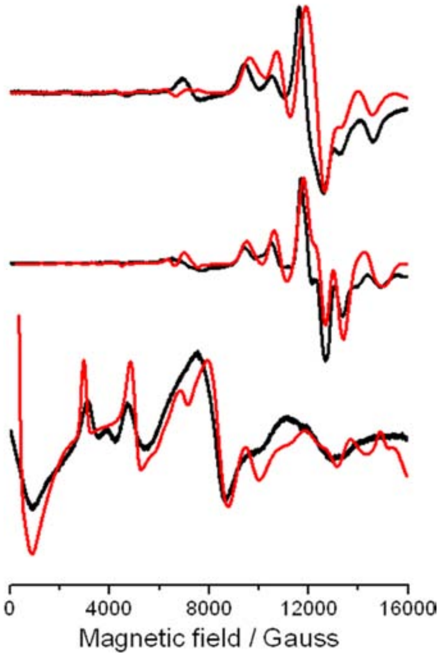

Figure 4. Q-band (ca. 34 GHz) EPR spectra of polycrystalline samples of **1** (top), **2** (middle), and **3** (bottom) at $T = 5$ K: experimental (black) and calculated (red), with the parameters in the text.

The fact that there is no evidence of a Mn···Mn interaction in the EPR spectrum of **1** means that the exchange coupling must be extremely weak. Several attempts were made to support the conclusion of very weak magnetic exchange in **1** by variable-temperature SQUID magnetometry experiments; however, the extreme air-sensitivity of **1** meant that it was not possible to obtain reliable data. Given that the $\{CpMnN_3\}$ coordination environment in **1** is much more closely related to the $\{CpMnN_2\}$ environment in **3** than to the $\{MnN_4\}$ environment in **2**, the similarity of $|D|$ for **1** and **2** is surprising. The near axiality of **1** is easier to explain: in contrast to the pseudo-C_{2v} $\{CpMnN_2\}$ environment in **3**, the six-coordinate pseudotetrahedral $\{CpMnN_3\}$ environment in **1** makes it nearer to trigonal (although the distortion of the three N-donors from C_{3v} is substantial).

■ CONCLUSION

The bis(imino)bis(amino)phosphate-manganese(II) complexes $[(\eta^5\text{-Cp})Mn(\mu\text{-}L^1H_2)]_2$ (**1**), $[Mn(L^2H_2)_2]\cdot THF$ (**2**·THF), and $[(\eta^5\text{-Cp})Mn(L^3H_2)]$ (**3**) were synthesized by monodeprotonation of (L^nH_3) by manganocene in toluene (**1** and **3**) or THF (**2**). Complexes **1** and **3**, which adopt the general formula $[(\eta^5\text{-Cp})Mn(\mu\text{-}L^nH_2)]_x$, with $x = 1$ (**1**) or 2 (**3**), reveal that the steric bulk of the N-substituents on the ligands plays an important role in determining aggregation state. The bulky *t*-butyl group in **3** precludes dimerization on steric grounds, whereas the *n*-propyl group in **1** has sufficiently low steric demands that dimerization is possible, which results in a higher valence electron count of 17. The intermediate steric demands of the cyclohexyl groups in **2** enable two of these ligands to coordinate to the same manganese(II) center, although the effects of using THF as the solvent may also influence the outcome of the reaction that results in **2**. The Q-band EPR spectra of **1**−**3** were recorded at 5 K, and were simulated on the basis of isolated high-spin manganese(II) centers ($S = {}^5/_2$) with $g = 2.00$. The values of the ZFS parameter D are typical of high-spin manganese(II); however, the magnitude of D in **3** was found to be much greater than the D values of **1** and **2**. Although antiferromagnetic exchange in polymetallic manganese(II) amides has been observed previously,[10,11] the EPR spectrum of the dimer **1** did not show any evidence of exchange, which suggests that such interactions must be extremely weak.

With only three examples, the diverse coordination behavior of imino-phosphate ligands toward manganese(II) is apparent. The use of imino analogues of oxygen-containing phosphorus(V) ligands more widely in transition metal chemistry is an underdeveloped area, and our ongoing research will pursue this topic.

■ EXPERIMENTAL SECTION

All syntheses were carried out using standard Schlenk techniques using an inert atmosphere of dinitrogen. THF was predried over sodium wire before being dried by refluxing over molten potassium. Toluene was dried using an Innovative Technology solvent purification system, and then stored over activated 4 Å molecular sieves. Cp_2Mn,[14] $Me_3SiN{=}PCl_3$,[15] and $Me_3SiN{=}P(NHR)_3$ (R = Cy, ^{t}Bu) were synthesized using literature procedures,[6b] and all other reagents were purchased and used as supplied. NMR spectra were recorded on a Bruker Avance III 400 MHz spectrometer operating at a temperature of 298 K and frequencies of 400.13 (^{1}H), 100.61 (^{13}C), and 161.97 MHz (^{31}P). Q-band EPR spectra were measured on a Bruker EMX spectrometer.

Synthesis of $Me_3SiN{=}P(NH^nPr)_3$ (L^1H_3). The method used to synthesize $Me_3SiN{=}P(NH^nPr)_3$ is essentially identical to that developed by Chivers for the cyclohexyl and *tert*-butyl analogues: $Me_3SiN{=}PCl_3$ (3.93 g, 17.5 mmol) was added dropwise to a stirred suspension of $LiNH^nPr$ (3.90 g, 60.0 mmol) in Et_2O (70 mL) at 0 °C. After 30 min, the reaction mixture was slowly warmed to room temperature and stirred for a further 18 h. A white precipitate formed, which was removed via filtration (Celite, P3), and the solvent was removed from the filtrate *in vacuo* to give a white powder. The white powder was recrystallized from pentane (20 mL), resulting in the formation of $Me_3SiN{=}P(NH^nPr)_3$ as colorless crystals (1.83 g, 6.3 mmol, 36%). ^{1}H NMR ($CDCl_3$, δ/ppm, J/Hz): 2.76, broad triplet, 6H, $CH_2CH_2CH_3$ $^3J = 8.0$; 2.01, broad singlet, 3H, NH; 1.44, sextet, 6H, $CH_2CH_2CH_3$ $^3J = 8.0$; 0.89, t, 9H $CH_2CH_2CH_3$ $^3J = 8.0$; −0.04, s, 9H, $SiMe_3$. ^{13}C NMR ($CDCl_3$, δ/ppm, J/Hz): 43.24, $CH_2CH_2CH_3$; 25.54, $CH_2CH_2CH_3$; 11.55, $CH_2CH_2CH_3$; 3.81, $SiMe_3$. ^{31}P NMR ($CDCl_3$, δ/ppm, J/Hz): 7.78. Anal. Calcd for $C_{12}H_{33}N_4PSi$: C 49.28, H 11.37, N 19.16. Found: C 49.41, H 10.98, N 19.09.

Synthesis of 1. A solution of Cp_2Mn (0.06 g, 0.3 mmol) in toluene (10 mL) was added to a stirred solution of $Me_3SiN{=}P(NH^nPr)_3$ (0.10 g, 0.3 mmol) in toluene (10 mL) at −78 °C. The dark brown solution was stirred for 30 min and then slowly warmed to room temperature, producing a green solution. The reaction was stirred for two hours and filtered (Celite, P3). Storage of the solution for six days at +2 °C produced green crystals of **1** (0.072 g, 60% based on manganese). Anal. Calcd for $C_{34}H_{74}Mn_2N_8P_2Si_2$: C 49.62, H 9.06, N 13.62. Found: C 49.78, H 9.43, N 13.35. ^{1}H NMR (C_6D_6, δ/ppm): very broad resonance extending from approximately +46 to −14 ppm, maximum at 17.1 ppm, overlaps with all other observed resonances, C_5H_5; 14.97, broad singlet, $SiMe_3$; resonances due to *n*-propyl groups observed at 14.29, 10.49, 9.91, 9.13, 8.14; NH protons not observed.

Synthesis of 2. A solution of Cp_2Mn (0.05 g, 0.2 mmol) in THF (10 mL) was added to a stirred solution of $Me_3SiN{=}P(NHCy)_3$ (0.20 g, 0.5 mmol) in THF (10 mL) at −78 °C. The dark brown solution was stirred for 30 min and then slowly warmed to room temperature upon which the solution turned orange-brown in color. The reaction was stirred for a further 18 h and then filtered (Celite, P3). The filtrate was reduced in volume until solid material began to be deposited on the walls of the Schlenk tune, and the solution was then stored at −5 °C. Pale brown crystals of **2** formed after five days (0.12 g, 56%). Anal. Calcd for $C_{42}H_{88}MnN_8P_2Si_2$: C 57.44, H 10.10, N 12.76. Found: C

Table 1. Crystal Data and Structure Refinement for **1**−**3**

	1	**2**	**3**
formula	$C_{34}H_{70}Mn_2N_8P_2Si_2$	$C_{42}H_{88}MnN_8P_2Si_2$	$C_{20}H_{43}MnN_4PSi$
fw	818.98	878.28	453.58
cryst syst	triclinic	monoclinic	orthorhombic
space group	$P\bar{1}$	$C2/c$	$Pmmn$
a/Å	10.4186(12)	24.6619(11)	11.366(2)
b/Å	10.8372(12)	10.9942(4)	11.833(3)
c/Å	10.9199(12)	21.8157(9)	9.4828(13)
α/deg	91.861(9)	90	90
β/deg	98.026(9)	90.494(4)	90
γ/deg	115.271(11)	90	90
V/Å^3	1098.2(2)	5914.8(4)	1275.4(4)
Z	2	1	2
cryst size/mm^3	0.21 × 0.15 × 0.10	0.33 × 0.30 × 0.15	0.30 × 0.20 × 0.20
θ range/deg	2.95−28.51	3.09−27.50	3.29−25.02
reflns collected	4717	6611	2986
indep reflns	2079	4680	1252
R(int)	0.2308	0.0559	0.0585
completeness/%	98.5	97.2	99.7
data/restraints/params	4717/0/223	6611/0/289	1252/184/121
GOF on F^2	0.777	1.033	1.054
final R indices $[I > 2\sigma(I)]$	R1 = 0.0548	R1 = 0.0669	R1 = 0.0640
	wR2 = 0.1099	wR2 = 0.1679	wR2 = 0.1561
R indices (all data)	R1 = 0.1343	R1 = 0.0904	R1 = 0.0928
	wR2 = 0.1365	wR2 = 0.1747	wR2 = 0.1776

57.34, H 9.96, N 12.72. ^{1}H NMR: 31.0, broad shoulder overlapping with adjacent resonances; 19.57, broad, overlapping with adjacent resonances; 14.14, broad, overlapping with adjacent resonances.

Synthesis of 3. A solution of Cp_2Mn (0.06 g, 0.3 mmol) in toluene (10 mL) was added to a stirred solution of $Me_3SiN{=}P(NH^tBu)_3$ (0.10 g, 0.3 mmol) in toluene (10 mL) at −78 °C. After 30 min, the dark brown solution was slowly warmed to room temperature, resulting in an amber solution. The solution was stirred for two hours, gently heated, and filtered while hot (Celite, P3). The resultant solution was reduced in volume and stored at −5 °C for seven days, giving amber crystals of **3** (0.047 g, 35%). Anal. Calcd for $C_{20}H_{43}Mn_1N_4PSi$: C 52.96, H 9.56, N 12.35. Found: C 52.82, H 9.46, N 12.24. ^{1}H NMR (C_6D_6, δ/ppm): 33.78, v broad, C_5H_5; 14.10, ^{t}Bu; 13.36, ^{t}Bu; 8.86 ^{t}Bu; 8.23, $SiMe_3$; NH protons not observed.

X-ray Crystallography. Crystallographic studies were carried out using an Oxford Diffraction XCalibur2 instrument. Data were collected at 100(2) K, and molybdenum radiation (λ = 0.710 73 Å) was used in each case. Full-matrix least-squares on F^2 was used to refine all structures. CCDC deposition numbers 884430−884432.

■ ASSOCIATED CONTENT

Ⓢ Supporting Information

X-ray crystallographic data on **1**−**3** in CIF format. This material is available free of charge via the Internet at http://pubs.acs.org.

■ AUTHOR INFORMATION

Corresponding Author

*E-mail: Richard.Layfield@manchester.ac.uk.

Author Contributions

The manuscript was written through contributions of all authors. All authors have given approval to the final version of the manuscript.

Notes

The authors declare no competing financial interest.

■ ACKNOWLEDGMENTS

R.A.L. thanks the Alexander von Humboldt Foundation for the award of a Fellowship for Experienced Researchers. The authors acknowledge the support of the EPSRC (U.K.). Dr. Madeleine Helliwell is acknowledged for assistance in refining the crystal structure of **3**.

■ REFERENCES

(1) (a) *Metal Phosphonate Chemistry: From Synthesis to Applications*; Clearfield, A., Demadis, K., Eds.; Royal Society of Chemistry Publishing: Cambridge, U.K., 2012. (b) Clearfield, A. *Dalton Trans.* **2008**, 6089.

(2) Chandrasekhar, V.; Senapati, T.; Dey, A.; Hossain, S. *Dalton Trans.* **2011**, *40*, 5394.

(3) (a) Iremonger, S. S.; Liang, J.; Vaidhyanathan, R.; Shimizu, G. K. H. *Chem. Commun.* **2011**, *47*, 4430. (b) Taylor, J. M.; Mah, R. K.; Moudrakovski, I. L.; Ratcliffe, C. I. *J. Am. Chem. Soc.* **2010**, *132*, 14055.

(4) (a) See, for example: Zheng, Y. Z.; Pineda, E. M.; Helliwell, M.; Winpenny, R. E. P. *Chem.—Eur. J.* **2012**, *18*, 4161. (b) Zheng, Y. Z.; Evangelisti, M.; Tuna, F.; Winpenny, R. E. P. *J. Am. Chem. Soc.* **2012**, *134*, 1057. (c) Zheng, Y. Z.; Evangelisti, M.; Winpenny, R. E. P. *Angew. Chem., Int. Ed.* **2011**, *50*, 3692. (d) Khanra, S.; Kloth, M.; Mansaray, H.; Muryn, C. A.; Tuna, F.; Sanudo, E. C.; Helliwell, M.; McInnes, E. J. L.; Winpenny, R. E. P. *Angew. Chem., Int. Ed.* **2007**, *46*, 5568.

(5) (a) Chivers, T.; Brask, J. K. *Angew. Chem., Int. Ed.* **2001**, *40*, 3960. (b) Aspinall, G. M.; Copsey, M. C.; Leddham, A. P.; Russell, C. A. *Coord. Chem. Rev.* **2002**, *227*, 217. (c) Steiner, A.; Zacchini, S.; Richards, P. *Coord. Chem. Rev.* **2002**, *227*, 193.

(6) (a) Chivers, T.; Krahn, M.; Parvez, M.; Schatte, G. *Chem. Commun.* **2001**, 1922. (b) Armstrong, A.; Chivers, T.; Krahn, M.; Parvez, M.; Schatte, G. *Chem. Commun.* **2002**, 2332. (c) Chivers, T.; Krahn, M.; Schatte, G.; Parvez, M. *Inorg. Chem.* **2002**, *42*, 3994. (d) Armstrong, A.; Chivers, T.; Krahn, M.; Parvez, M.; Schatte, G.; Boeré, R. T. *Inorg. Chem.* **2004**, *43*, 3453. (e) Armstrong, A.; Chivers, T.; Parvez, M.; Boeré, R. T. *Angew. Chem., Int. Ed.* **2004**, *43*, 502. (f) Armstrong, A.; Chivers, T.; Krahn, M.; Parvez, M. *Can. J. Chem.* **2005**, *83*, 1768.

(7) (a) Bickley, J. F.; Copsey, M. C.; Jeffrey, J. C.; Leedham, A. P.; Russell, C. A.; Stalke, D.; Steiner, A.; Stey, T.; Zacchini, T. *Dalton Trans.* **2004**, 989. (b) Raithby, P. R.; Russell, C. A.; Steiner, A.; Wright, D. S. *Angew. Chem., Int. Ed.* **1997**, *36*, 649.

(8) (a) Rufanov, K. A.; Ziemer, B.; Meisel, M. *Dalton Trans.* **2004**, 3808. (b) Scherer, O.; Kerth, J.; Sheldrick, W. S. *Angew. Chem., Int. Ed.* **1984**, *23*, 156.

(9) Layfield, R. A. *Chem. Soc. Rev.* **2008**, *37*, 1098.

(10) (a) Alvarez, C. S.; Boss, S. R.; Burley, J. C.; Humphrey, S. M.; Layfield, R. A.; Kowenicki, R. A.; McPartlin, M.; Rawson, J. M.; Wheatley, A. E. H.; Wood, P. T.; Wright, D. S. *Dalton Trans.* **2004**, 3481. (b) Alvarez, C. S.; Bond, A. D.; Harron, E. A.; Layfield, R. A.; Mosquera, M. E. G.; McPartlin, M.; Rawson, J. M.; Wright, D. S. *Dalton Trans.* **2003**, 3002. (c) Alvarez, C. S.; Bond, A. D.; Cave, D.; Mosquera, M. E. G.; Harron, E. A.; Layfield, R. A.; McPartlin, M.; Rawson, J. M.; Wood, P. T.; Wright, D. S. *Chem. Commun.* **2002**, 2980. (d) Alvarez, C. S.; Bond, A. D.; Harron, E. A.; Layfield, R. A.; McAllister, J. A.; Pask, C. M.; Rawson, J. M.; Wright, D. S. *Organometallics* **2001**, *20*, 4135.

(11) (a) Köhler, F. H.; Hebendanz, N.; Müller, G.; Thewalt, U. *Organometallics* **1987**, *6*, 115. (b) Köhler, F. H.; Hebendanz, N.; Thewalt, U.; Kanellakopulos, B.; Klenze, R. *Angew. Chem., Int. Ed.* **1984**, *23*, 721.

(12) (a) Stokes, F. A.; Less, R. J.; Haywood, J.; Melen, R. L.; Thompson, R. I.; Wheatley, A. E. H.; Wright, D. S. *Organometallics* **2012**, *31*, 23. (b) Krinsky, J. L.; Stavis, M. N.; Walter, M. D. *Acta Crystallogr.* **2003**, *E59*, m497. (c) Bashall, A.; Beswick, M. A.; Ehlenberg, H.; Kidd, S. J.; McPartlin, M.; Palmer, J.; Raithby, P. R.; Rawson, J. M.; Wright, D. S. *Chem. Commun.* **2000**, 749. (d) Heck, J.; Massa, W.; Weinig, P. *Angew. Chem., Int. Ed.* **1984**, *23*, 722. (e) Scheuermayer, S.; Tuna, F.; Bodensteiner, M.; Scheer, M.; Layfield, R. A. *Chem. Commun.* **2012**, *48*, 8087.

(13) Howard, C. G.; Girolami, G. S.; Wilkinson, G.; Thornton-Pett, M.; Hursthouse, M. B. *J. Am. Chem. Soc.* **1984**, *106*, 2033.

(14) Wilkinson, G.; Cotton, F. A.; Birmingham, J. M. *J. Inorg. Nucl. Chem.* **1956**, *2*, 95.

(15) Wang, B.; Rivard, E.; Manners, I. *Inorg. Chem.* **2002**, *41*, 1690.